

Chandra reveals a black-hole X-ray binary within the ultraluminous supernova remnant MF 16

T. P. Roberts^{1,*} & E. J. M. Colbert²

¹ *X-ray and Observational Astronomy Group, Dept. of Physics & Astronomy, University of Leicester, University Road, Leicester, LE1 7RH*

² *Department of Physics and Astronomy, Johns Hopkins University, Baltimore, MD 21218, USA*

**E-mail: tro@star.le.ac.uk*

ABSTRACT

We present evidence, based on *Chandra* ACIS-S observations of the nearby spiral galaxy NGC 6946, that the extraordinary X-ray luminosity of the MF 16 supernova remnant actually arises in a black-hole X-ray binary. This conclusion is drawn from the point-like nature of the X-ray source, its X-ray spectrum closely resembling the spectrum of other ultraluminous X-ray sources thought to be black-hole X-ray binary systems, and the detection of rapid hard X-ray variability from the source. We briefly discuss the nature of the hard X-ray variability, and the origin of the extreme radio and optical luminosity of MF 16 in light of this identification.

Key words: Galaxies: individual: NGC 6946 – X-rays: binaries – ISM: supernova remnants

1 INTRODUCTION

An observational definition of ultraluminous X-ray sources (ULX) is those X-ray sources detected coincident with nearby galaxies, that are both located outside the galactic nucleus and display an observed luminosity in excess of 10^{39} erg s⁻¹. There has recently been a lot of attention paid to this class of object based on the argument that if they are accretion-powered systems, then in many cases the observed X-ray luminosity exceeds the Eddington luminosity for a 10 M_⊙ black hole. Explanations for this apparent breach of the Eddington limit include accretion on to a new class of $10^2 - 10^5$ M_⊙ *intermediate-mass* black hole (e.g. Colbert & Mushotzky 1999; Miller & Hamilton 2002), super-Eddington radiation from bloated accretion discs in X-ray binaries (Begelman 2002), and anisotropic emission from X-ray binaries (e.g. King et al. 2001; Körding, Falcke & Markoff 2002; King 2002).

However, not all ULX are accreting systems. A minority are actually recent supernovae, such as SN 1986J (Bregman & Pildis 1992), SN 1979C (Immler, Pietsch & Aschenbach 1998), SN 1978K (Ryder et al. 1993) and SN 1995N (Fox et al. 2000) to name but four. Such objects have been observed to reach X-ray luminosities of 10^{41} erg s⁻¹ (e.g. SN 1988Z, Fabian & Terlevich 1996) and are thought to be the result of the supernova exploding into a dense circumstellar environment. The ULX phase for young supernova remnants can be short, however, with many (though not all) showing steep X-ray flux decay curves (Immler & Lewin 2002). Reports of much older, evolved supernova remnants with ULX-like fluxes, for instance the “hypernova” remnants of M101

(Wang 1999), have since turned out to be mis-identifications of X-ray binaries (Snowden et al. 2001).

One supernova remnant that appears to have remained unusually X-ray luminous whilst becoming quite evolved is the remnant MF 16 in NGC 6946 (nomenclature from Mattonick & Fesen 1997). Though the X-ray source was detected in an *Einstein* IPC observation of NGC 6946 (Fabbiano & Trinchieri 1987), it was first identified as an extremely X-ray luminous supernova remnant ($L_X \sim 3 \times 10^{39}$ erg s⁻¹ at 5.1 Mpc, placing it firmly in the ULX regime) on the basis of *ROSAT* PSPC data (Schlegel 1994). The X-ray data appeared consistent with a young supernova remnant, but optical data revealed the remnant to be evolved, possibly ~ 3500 years old (Blair & Fesen 1994). The remnant appears extraordinarily luminous in X-rays, optical line emission and radio continuum emission (van Dyk et al. 1994) for a supernova remnant of this age. Subsequent *HST* observations revealed MF 16 to have a physical size of $\sim 34 \times 20$ pc, and a distinct morphology characterised by three “loops” apparent in narrow-band H α and [SII] images (Blair, Fesen & Schlegel 2001; hereafter BFS01), though an [OIII] image suggested a more elliptical structure with a possible young star at the heart of the nebula. In conjunction with optical spectral data, BFS01 suggest that the extraordinary luminosity of this remnant is due to the blast wave of a young supernova impacting on the dense shell of an older remnant. *ROSAT* and *ASCA* data were used to investigate the X-ray emission in detail by Schlegel, Blair & Fesen (2000), who found the spectral data to fit well to a dual Raymond-Smith thermal plasma model. This is consistent with the *HST* data if the hot component comes from the interaction zone and

Table 1. Details of the *Chandra* observations.

Sequence number	Aimpoint (J2000)	Date	Exposure (ks)
500109	20 ^h 34 ^m 49.0 ^s , +60°09′19″	2001-09-07	58.3
500406	20 ^h 34 ^m 51.2 ^s , +60°09′16″	2002-11-25	30.0

the soft component from within the supernova bubble. An alternate view is offered by Dunne, Gruendl & Chu (2000), who propose that the remnant originates in the interaction of a single supernova blast wave with a dense circumstellar nebula ejected from a massive progenitor star. They suggest that a hard component in the *ROSAT* PSPC spectral data may originate in a pulsar wind nebula.

The first of the two *Chandra* observations reported in this letter has been presented by Holt et al. (2003). They conclude that the featureless X-ray spectrum of MF 16 excludes the interaction of a blast wave with circumstellar matter, and does not appear to fit to a pulsar wind nebula model either. They suggest that the X-ray emission may originate in an unusual, if not unique, set of circumstances. Here, we re-analyse this data in tandem with a later public observation of NGC 6946, and demonstrate that the X-ray source associated with MF 16 is in fact a black-hole X-ray binary (BHXR), explaining the apparent dichotomy of an evolved remnant with a young supernova-like X-ray flux.

2 OBSERVATIONS & DATA REDUCTION

NGC 6946 has been observed by *Chandra* on two separate occasions. The details of the observations are given in Table 1. Both observations were pointed at its nuclear region, though the target of the latter observation was the recent supernova SN2002HH, and the large majority of the area of the galaxy falls on the ACIS-S3 chip. MF 16 lies about 2.5 arcmin north-east of the observation aimpoint, fortuitously on the S3 chip in both datasets.

The data was reduced and subsequently analysed using the CIAO v2.3 and HEASoft v5.2 packages. The level 2 event lists were initially filtered down to an energy range of 0.3 – 10 keV, and images were created at the full detector spatial resolution (1 pixel \equiv 0.492 arcsec). Source spectra and lightcurves were then extracted using the PSEXTRACT and LIGHTCURVE tools respectively, from within a 10-pixel radius circular aperture set to encompass the full point spread function of the X-ray source. Background regions were extracted from a similar-size aperture displaced by \sim 10 arcsec from MF 16. Neither event list was time-filtered for background flaring, as the total background measured from the unfiltered background regions amounted to less than 0.5% of the counts accumulated from the source in either observation, allowing us to exploit the full exposure time.

3 EVIDENCE THAT MF 16 CONTAINS AN X-RAY BINARY SYSTEM

The X-ray counterpart of MF 16 (hereafter NGC 6946 X-11, after Roberts & Warwick 2000) was detected in both observations as the brightest X-ray source on the *Chandra* ACIS-

S3 chip, at a position 20^h35^m00.75^s, +60°11′30.9″¹. A total of 8585 ± 94 and 3838 ± 63 counts were detected from the source in the 2001 September and 2002 November observations respectively. This is currently amongst the largest datasets for an ULX in the *Chandra* era. In the following sections we present the details of its X-ray characteristics.

3.1 Spatial

We test whether NGC 6946 X-11 is spatially extended by comparing its radial profile from the 2001 September observation to a modelled point spread function (PSF) for a point-like X-ray source at the same detector position and off-axis angle². The model is interpolated from a library of model PSFs using the MKPSF tool, at an energy of 1.5 keV. We account for known residual aspect correction errors (c.f. section 2.2 of Zezas et al. 2002) by convolving the model PSF with a 2-D Gaussian function of HWHM = 0.75 arcsec. Radial profiles for the model and source data were extracted in one-pixel width annuli around the source centroid, and the model PSF was normalised to the same central peak as the source. Approximating the PSF shape by a Gaussian function showed the source data and the modelled PSF to match extraordinarily well, with the best fit to each giving a HWHM of 1.31 ± 0.02 arcsec for the data, and 1.33 ± 0.02 arcsec for the model (the fitting was performed using a χ^2 minimization algorithm, and the errors quoted are 90% errors for one interesting parameter). The observed X-ray emission is therefore fully consistent with originating in a point-like source. However, by comparison with Roberts et al. (2002) we note that on-axis Gaussian fits to point-like sources give a HWHM of \sim 1 arcsec for a spatial resolution of 0.5 arcsec. Scaling this to our observation implies it is sensitive to structure on scales of $>$ 0.7 arcsec, ruling out extended X-ray emission on the full scale of MF 16 (1.4×0.8 arcsec²; BFS01), though some spatial extension on scales less than this cannot be excluded.

3.2 Spectral

Before undergoing spectral analysis, the auxilliary response files for both datasets were corrected for the known quantum efficiency degradation of the ACIS-S3 chip using the CORRARF tool. The extracted source spectra were binned to a minimum of 20 counts per bin before analysis in XSPEC v11.2, and only data in bins located above an energy of 0.5 keV were considered. The observed 0.3 – 10 keV count rates of \sim 0.12 – 0.14 count s⁻¹ were accumulated in a full-frame exposure mode in both observations which, even allowing for their off-axis positions, implies that the source data will have suffered from a moderate level (\sim 10 – 15%) of pile-up. We account for this in the following analysis using the XSPEC v11.2 parameterisation of the Davis (2001) CCD pile-up mitigation algorithm.

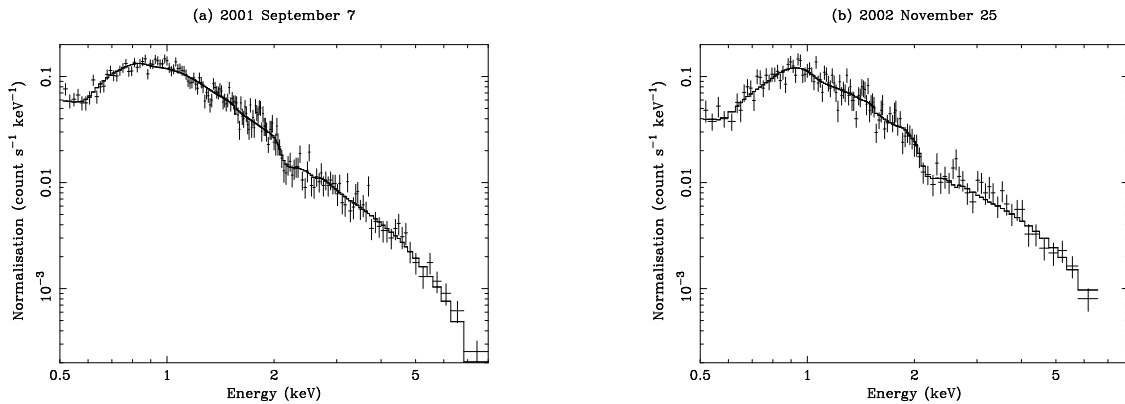
¹ This is an average of the two positions from the separate observations, though the difference between the measured positions was a mere 0.4″.

² Combining the data from both observations to produce a higher quality radial profile is not an option, since the source is at different off-axis angles and detector positions in the two observations.

Table 2. Two-component fits to the *Chandra* X-ray spectral data.

Model ^a	Epoch ^b	α^c	N_H ($\times 10^{22}$ cm ⁻²)	kT_1 (keV)	Abundance (Solar units)	kT_{in} (keV)	Γ	kT_2 (keV)	χ^2/dof
PU*WA*(D+PO)	A	$0.16^{+0.06}_{-0.04}$	$0.37^{+0.04}_{-0.02}$	-	-	0.16 ± 0.01	$2.53^{+0.09}_{-0.14}$	-	178.0/155
	B	< 0.19	$0.47^{+0.1}_{-0.08}$	-	-	0.14 ± 0.01	$2.28^{+0.18}_{-0.21}$	-	127.9/112
PU*WA*(B+PO)	A	$0.16^{+0.06}_{-0.04}$	$0.38^{+0.09}_{-0.06}$	$0.12^{+0.01}_{-0.02}$	-	-	$2.46^{+0.07}_{-0.21}$	-	183.9/155
	B	< 0.31	$0.44^{+0.05}_{-0.11}$	0.12 ± 0.01	-	-	2.23 ± 0.22	-	128.3/112
PU*WA*(M+PO)	A	$0.38^{+0.04}_{-0.08}$	0.2^f	$0.66^{+0.13}_{-0.07}$	> 7.4	-	$2.49^{+0.05}_{-0.06}$	-	183.4/155
	B	$0.30^{+0.07}_{-0.15}$	0.2^f	$0.77^{+0.08}_{-0.15}$	$5.7^{+3.0}_{-4.0}$	-	$2.32^{+0.1}_{-0.13}$	-	123.3/112
PU*WA*(M+M)	A	$0.42^{+0.15}_{-0.04}$	0.2^f	0.33 ± 0.02	0.07 ± 0.01	-	-	2.15 ± 0.12	200.6/155
	B	$0.34^{+0.07}_{-0.02}$	0.2^f	0.64 ± 0.05	$0.14^{+0.01}_{-0.04}$	-	-	$2.43^{+0.78}_{-0.69}$	135.4/112

Notes: ^a Model components are: PU - pileup correction; WA - cold absorption; D - multicolour disc blackbody; PO - powerlaw continuum; B - classical blackbody; M - MEKAL optically thin thermal plasma model. ^b Epoch of observation, with A \equiv 2001 September and B \equiv 2002 November. ^c Grade migration parameter in the pile-up mitigation model. ^f Parameter value fixed at that shown.


Figure 1. The observed X-ray spectra (data points) and best fitting models (solid lines; c.f. Table 2) from the *Chandra* observations of NGC 6946 X-11. The datasets are plotted on identical axes for direct comparison.

Neither dataset was well-fit by a variety of single-component simple models, with an absorbed powerlaw continuum the only model to have a reduced- χ^2 value below 2 for both datasets. We note that in both cases a correction for pile-up was justified since it provided an improvement to the fit at a significance of > 99.8% for one extra degree of freedom, though the resulting fits were still poor ($\chi^2/\text{dof} = 239.8/157$ and $159.2/114$ for the 2001 September and 2002 November observations respectively).

The fits to the data were greatly improved by the addition of a second spectral component to the absorbed powerlaw continuum model. We show the models and best fit parameters in Table 2. All errors are quoted as the 90% error for one interesting parameter. The additional component required to improve the fit turned out in all cases to be a very soft component, which could be modelled by either a multicolour disc blackbody (hereafter MCDBB; Mitsuda et al. 1984) with an inner-disc temperature of $kT_{in} \sim 0.15$ keV, a classical blackbody emission spectrum of temperature $kT \sim 0.12$ keV, or a MEKAL optically thin thermal plasma model with $kT \sim 0.7$ keV. The resulting goodness of fit (as measured by the χ^2/dof) was remarkably similar for all three models in each epoch, with the model containing the MCDBB component marginally preferred in the first epoch, and the model including the MEKAL in the second. We show the data and the corresponding best-fitting model for both observations in Figure 1. We note, however, that to

constrain a best fit using the MEKAL plus powerlaw model the line-of-sight column densities had to be fixed to a minimum value equal to the foreground column through our own galaxy ($\sim 2 \times 10^{21}$ atoms cm⁻²; interpolated from the HI maps of Stark et al. 1992). This seems physically implausible, since the observation of no absorption intrinsic to MF 16 is at odds with the total extinction of $E(B - V) = 0.65$ observed for its optical emission lines (BFS01). This extinction converts to a column of 4.3×10^{21} atoms cm⁻² (c.f. Zombeck 1990).

On the other hand, the MCDBB or classical blackbody plus powerlaw continuum model fits are consistent with the inferred column to the central regions of MF 16. Crucially, the MCDBB plus powerlaw continuum model has recently been found to describe the *Chandra* or *XMM-Newton* X-ray spectra of several ULX that are known or suspected BHXRB (e.g. Miller et al. 2003). Furthermore, the derived parameters, and in particular the inner-disc temperature and normalisation (constrained at 870^{+660}_{-170} and 1600^{+1700}_{-1300} km⁻² (10 kpc)⁻² in epochs A and B respectively) of the MCDBB appear extraordinarily similar when our fits are compared to the ULX studied by Miller et al. (2003). This suggests that the X-ray emission processes in NGC 6946 X-11 are those of a BHXRB. The data also suggest that the spectrum changes between observations, though as the error ranges for each of the parameters overlap none of the changes are very statistically significant. This tentative suggestion of spectral

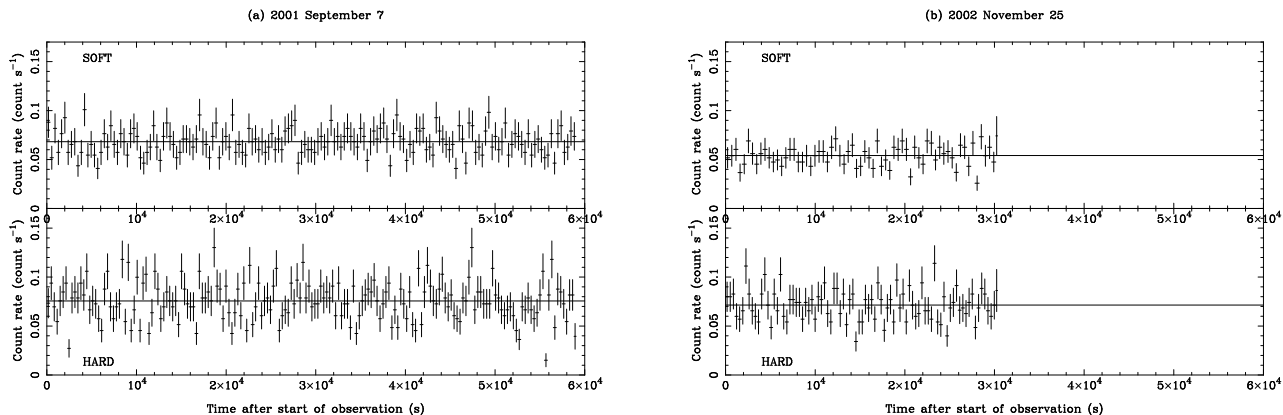


Figure 2. *Chandra* lightcurves for NGC 6946, split into soft (0.3 – 1.1 keV; top panel) and hard (1.1 – 10 keV; lower panel) X-ray emission. Each panel is plotted on identical axes for direct comparison.

variation is also indicative of BXR behaviour. We note that the observed 0.5 – 8 keV luminosity of NGC 6946 X-11 from this model is $\sim 2.5 \times 10^{39}$ erg s^{-1} , of which $\sim 20\%$ originates in the MCDBB component.

Finally, we also fit a dual MEKAL model to the data, similar to the dual Raymond-Smith plasma model used to provide a fit to the combined *ROSAT* PSPC/*ASCA* spectral data (Schlegel, Blair & Fesen 2000). We are again required to constrain the absorption column to the foreground galactic value. Our fits provide reasonably similar results to the low-Z *ROSAT* PSPC/*ASCA* fit, albeit with our substantially lower fit abundances allowing the temperatures of both components to be lower in the *Chandra* data. However, this model is clearly the least preferred of the four two-component spectral models for both *Chandra* datasets, arguing that the blast wave interaction interpretation of Schlegel, Blair & Fesen (2000) is not favoured by the *Chandra* data.

3.3 Temporal

Previous analyses of this object have suggested that the X-ray flux remains constant over a timescale of years (e.g. Holt et al. 2003), as would be expected for the X-ray emission from an object up to 30 pc in diameter. Here, we detect a drop of $\sim 13\%$ in the 0.3 – 10 keV count rate over a year, from 0.144 count s^{-1} to 0.125 count s^{-1} , clearly inconsistent with such an extended X-ray source. However, the *Chandra* CCDs have a known problem with their quantum efficiency, and hence effective area to incoming photons, degrading with time. This could lead to drops in the detected count rate for separate observations of constant X-ray fluxes, particularly for sources with soft X-ray spectra. We checked this by running simulations in XSPEC, using the best fit model to the 2001 September data, and the auxiliary response file (corrected to the degraded area) from the 2002 November observation. An overall drop of $\sim 3\%$ in the count rate was predicted, clearly smaller than the observed deficit, implying that the source displays at least small amplitude variability on long timescales.

The X-ray variability was further investigated by deriving short-term lightcurves from both observations. Both lightcurves were extracted in the full 0.3 – 10 keV range and binned to a temporal resolution equivalent to 25 counts per

bin for a constant source count rate, in order to maximise the temporal resolution whilst maintaining a reasonable average signal-to-noise ratio of five per bin. Two simple tests for variability were then applied to these lightcurves. Firstly, a classic standard deviation of the count rate per bin from the mean count rate over the course of the observation was calculated, and then compared to the expected deviation of $\pm 20\%$ expected from Gaussian counting noise. Secondly, a χ^2 test was performed against the hypothesis that the source count rate remained constant during the observation. The results of these tests, including a probability that the data is variable, $P(\text{var})$, shown for the cases where it exceeds 90%, and the binning of the lightcurves are reported in Table 3. They show that the full band lightcurve for the 2002 November observation was statistically consistent with a flat count rate. However, both a large excess in the standard deviation and in the χ^2 statistic show the 2001 September data to be variable to very high probabilities (99.7 and $> 99.9\%$ likelihood, respectively). We investigated this variability further by splitting each dataset into two arbitrary energy bands containing approximately the same number of counts, a 0.3 – 1.1 keV “soft” band and a 1.1 – 10 keV “hard” band. The lightcurves for these bands are shown in Figure 2, again binned to the equivalent of an average of 25 counts per bin (c.f. Table 3 for actual bin sizes). Both the tests on the binned lightcurves show no strong evidence for variability in the soft band. However, strong evidence for variability is present in the hard band lightcurve in the 2001 September observation (at over 99.9% likelihood in both tests), and may also be present in the 2002 November observation ($\sim 96\%$ likelihood according to the χ^2 test).

In order to provide a separate test of the variability free of any gross photon binning effects we employed a Kolmogorov-Smirnov test, in which we compared the cumulative photon arrival times to the expected cumulative arrival times for a constant-flux source³. This provided separate confirmation of the strong variability in the 2001 September hard band data, and possible variability in the

³ Though note that the data is strictly limited by the 3.24104 s temporal resolution (which is the sum of the exposure time plus the frame readout time) of the ACIS-S3 chip in the course of performing this test.

Table 3. Tests of the short-term variability of NGC 6946 X-11.

Epoch	Band ^a	Bin size (s)	Standard deviation, σ		P_σ (var)	χ^2 statistic		K-S statistic P_{K-S} (var)
			Expected ^b	Observed ^b		χ^2/dof	P_{χ^2} (var)	
2001 September	Full	174	2.88×10^{-2}	$(3.37 \pm 0.18) \times 10^{-2}$	99.7%	534/340	> 99.9%	~ 94%
	Soft	367	1.36×10^{-2}	$(1.38 \pm 0.11) \times 10^{-2}$	-	145/160	-	-
	Hard	330	1.51×10^{-2}	$(1.97 \pm 0.15) \times 10^{-2}$	99.9%	402/178	> 99.9%	> 99%
2002 November	Full	199	2.51×10^{-2}	$(2.65 \pm 0.22) \times 10^{-2}$	-	158/152	-	-
	Soft	464	1.08×10^{-2}	$(1.03 \pm 0.13) \times 10^{-2}$	-	69/65	-	> 99%
	Hard	351	1.43×10^{-2}	$(1.55 \pm 0.17) \times 10^{-2}$	-	110/86	~ 96%	~ 95%

Notes: ^a as defined in the text. ^b in count s⁻¹. We only show P (var) in the instances where it highlights the variability.

2002 November hard data. Interestingly, it also showed the 2002 November soft data to be variable at very high significance (> 99%), which was not picked up by any other test. An examination of the photon arrival time distribution for the data shows this result is due to a very slight increase in the average soft count rate over the latter stages of the 2002 November observation, when compared to the earlier stages, which the standard deviation and χ^2 tests were insensitive to. The actual average count rate change was from $(5.25 \pm 0.17) \times 10^{-2}$ count s⁻¹ in the first 18.5 ks to $(5.61 \pm 0.22) \times 10^{-2}$ count s⁻¹ in the latter 11.5 ks. We note this is probably a real change, and is certainly not due to a change in the background count rate for the source, which remains at $\sim 10^{-4}$ count s⁻¹ in the soft band throughout the observation.

Our statistical tests, and the amplitude of the variability shown by Figure 2, demonstrate that the majority of the hard X-ray emission of NGC 6946 X-11 is varying at least on the timescale of the binning size we use to maximise our statistics, $\sim 330 - 350$ s. The hard X-ray emission is therefore originating in a region with a light crossing time of less than six minutes ($\approx 10^8$ km). This is consistent with a compact accretion-driven X-ray source such as an X-ray binary, and not with a spatially-extended supernova remnant. Note, however, that we cannot currently exclude the majority of the soft X-ray emission from originating in a more widespread component.

4 DISCUSSION

NGC 6946 X-11 is a point-like X-ray source, its X-ray spectrum is well-fit by models used to describe ultraluminous BHXRB, and its hard X-ray emission varies on timescales of less than six minutes. The simplest interpretation of this evidence is that the extraordinary X-ray luminosity of NGC 6946 X-11 originates in the accretion of matter in a BHXRB system, and not from the interaction of supernova blast waves with circumstellar material, or a pulsar wind nebula, as previously suggested. Of course, we cannot exclude some spatial extension in the X-ray source, which the lightcurves tell us would have to be soft X-ray emission. If we ignore for a moment the unrealistically low column to the MEKAL plus powerlaw continuum model, the MEKAL could still describe the hot gas phase of a supernova remnant. However, the spectral modelling implies that only $\lesssim 10\%$ of the observed flux originates in the MEKAL component, implying that the contribution to the observed luminosity from a hot plasma is limited to $\sim 2.5 \times 10^{38}$ erg s⁻¹.

If we are dealing with an ultraluminous BHXRB, it appears quite typical for the limited knowledge we have of this exotic class of object. A similar spectral model has been derived for the few other ULX with reasonable quality X-ray spectral data (Miller et al. 2003; Krauss et al. 2003; Kaaret et al. 2003), with the low inner-disc temperatures for the MCDDBB component interpreted as possible evidence for the presence of intermediate-mass black holes. We also note that the dominant powerlaw continuum component has a value very similar to that observed for Galactic BHXRBs in the high state (~ 2.5 ; c.f. Ebisawa, Titarchuk & Chakrabati 1996). One curious feature we have identified is that the X-ray variability in this ULX is predominantly above 1.1 keV, implying that it is the powerlaw continuum spectral component that is varying, and not the thermal emission from the accretion disc. This exclusively hard X-ray variability could quite conveniently explain the observed spectral hardening with increased flux seen in many ULX (e.g. Fabbiano et al. 2003). However, the scenario they describe where the hardening is due to a hotter inner accretion disc at higher accretion rates may not be consistent with our observations, due to the short variability timescales and the softness of the thermal disc component in the X-ray spectrum. The rapid variation of the hard X-rays may instead originate in other physical mechanisms, for instance variations at the base of a jet (c.f. Georganopoulos, Aharanion & Kirk 2002), or magnetic reconnection events in the accretion disc corona (c.f. Reeves et al. 2002 for a discussion of the latter mechanism applied to the quasar PDS 456).

Now that we have identified the X-ray emission from MF 16 with a BHXRB, where does this leave the physical models for the extreme radio and optical luminosity of the supernova remnant? It may be possible that the radio emission could originate from the BHXRB in a relativistically-beamed jet, similar to that reported for an ULX in NGC 5408 by Kaaret et al. (2003). It is also quite possible that the optical line emission may be a result of the presence of the BHXRB; we note that nebulae have been reported to be present at or around the positions of several ULX by Pakull & Mirioni (2003a,b). Some of these nebulae are present as giant ($d \sim 100 - 400$ pc) bubbles encircling the ULX position; they may be supernova remnants related to the birth of the ULX, as could be the case around IC 342 X-1 (see also Roberts et al. 2003), or may be inflated by the winds from young stars or relativistic jets from the BHXRB. Other nebulae, such as that present near the Holmberg II ULX, shows signs of X-ray ionization. We note that two of the key diagnostics of X-ray ionization, the presence of a He

II $\lambda 4686$ emission line (c.f. Pakull & Angebault 1986) and an abnormally high [OIII]/ $H\beta$ ratio (Remillard, Rappaport & Macri 1995) are present in the optical spectrum of MF 16 presented by BFS01. The similarity between MF16 and other ULX nebulae is noted by Pakull & Mirioni (2003b); we suggest here that at least some of the extraordinary optical emission-line luminosity of MF 16 may originate in X-ray excitation. Furthermore, we speculate that the nebula itself may be a young precursor of the giant bubbles seen by Pakull & Mirioni (2003a,b) around other ULX systems. Further studies of MF 16 in this context would be of great interest. Finally, we note that the *HST* images of MF 16 suggest the presence of a young stellar object at the centre of the nebula. Young stars or stellar clusters have been discovered coincident with at least two other ULX (Goad et al. 2002; Liu et al. 2002), hence it is possible that this object may be the optical counterpart of the BHXRB itself.

ACKNOWLEDGMENTS

The authors the referee, Eric Schlegel, for his useful comments that helped to improve this paper. We also thank Andy Ptak for assisting us in the use of XASSIST. TPR thanks Bob Warwick and Graham Wynn for useful discussions, and PPARC for financial support.

REFERENCES

- Begelman M.C., 2002, ApJ, 568, L97
 Blair W.P., Fesen R.A., 1994, ApJ, 424, L103
 Blair W.P., Fesen R.A., Schlegel E.M., 2001, AJ, 121, 1497 (BFS01)
 Bregman J.N., Pildis R., 1992, ApJ, 398, L107
 Colbert E.J.M., Mushotzky R.F., 1999, ApJ, 519, 89
 Davis J.E., 2001, ApJ, 562, 575
 Dunne B.C., Gruendl R.A., Chu Y.-H., 2000, AJ, 119, 1172
 Ebisawa K., Titarchuk L., Chakrabati S.K., 1996, PASJ, 48, 59
 Fabian A.C., Terlevich R., 1996, MNRAS, 280, L5
 Fabbiano G., Trinchieri G., 1987, ApJ, 315, 46
 Fabbiano G., Zezas A., King A.R., Ponman T.J., Rots A., Schweizer F., 2003, ApJ, 584, L5
 Fox D.W., et al., 2000, MNRAS, 319, 1154
 Georganopoulos M., Aharonian F., Kirk J., 2002, A&A, 388, L25
 Goad M.R., Roberts T.P., Knigge C., Lira P., 2002, MNRAS, 335, L67
 Holt S.S., Schlegel E.M., Hwang U., Petre R., 2003, ApJ, in press
 Immler S., Lewin W.H.G., 2002, astro-ph/0202231
 Immler S., Pietsch W., Aschenbach B., 1998, A&A, 331, 601
 Kaaret P., Corbel S., Prestwich A.H., Zezas A., 2003, Science, 299, 365
 King A., 2002, MNRAS, 335, L13
 King A., Davies M.B., Ward M.J., Fabbiano G., Elvis M., 2001, ApJ, 552, L109
 Körding E., Falcke H., Markoff S., 2002, A&A, 382, L13
 Krauss M., Kilgard R., Garcia M., Roberts T.P., Prestwich A., 2003, ApJ, submitted
 Liu J.-F., Bregman J.N., Seitzer P., 2002, ApJ, 580, L31
 Matonick D.M., Fesen R.A., 1997, ApJS, 112, 49
 Miller J.M., Fabbiano G., Miller M.C., Fabian A.C., 2003, ApJ, 585, L37
 Miller M.C., Hamilton D.P., 2002, MNRAS, 330, 232
 Mitsuda K., et al., 1984, PASJ, 36, 741
 Pakull M.W., Angebault L.P., 1986, Nature, 322, 511
 Pakull M.W., Mirioni L., 2003a, in Proceedings of the Symposium “New Visions of the Universe in the *XMM-Newton* and *Chandra* era”, ed. F. Jansen, ESA SP-488, astro-ph/0202488
 Pakull M.W., Mirioni L., 2003b, RMxAA, 15, 197
 Reeves J.N., Wynn G., O’Brien P.T., Pounds K.A., 2002, MNRAS, 336, L56
 Remillard R.A., Rappaport S., Macri L.M., 1995, ApJ, 439, 646
 Roberts T.P., Goad M.R., Ward M.J., Warwick R.S., 2003, MNRAS, in press
 Roberts T.P., Warwick R.S., 2000, MNRAS, 315, 98
 Roberts T.P., Warwick R.S., Ward M.J., Murray S.S., 2002, MNRAS, 337, 677
 Ryder S., Staveley-Smith L., Dopita M., Petre R., Colbert E.J.M., Malin D., Schlegel E., 1993, ApJ, 416, 167
 Schlegel E.M., 1994, ApJ, 424, L99
 Schlegel E.M., Blair W.P., Fesen R.A., 2000, AJ, 120, 791
 Snowden S., Mukai K., Pence W., Kuntz K., 2001, AJ, 121, 3001
 Stark A., Gammie C.F., Wilson R.W., Bally J., Linke R.A., Heiles C., Hurwitz M., 1992, ApJS, 79, 77
 van Dyk S.D., Sramek R.A., Weiler K.W., Hyman S.D., Virden R.E., 1994, ApJ, 425, L77
 Wang Q.D., 1999, 517, L27
 Zezas A., Fabbiano G., Rots A., Murray S., 2002, ApJ, 577, 710
 Zombeck M.V., 1990, Handbook of Astronomy and Astrophysics, Second Edition (Cambridge, UK: CUP)